京都大学防災研究所年報 第 50 号 B 平成 19 年 4 月
Annuals of Disas. Prev. Res. Inst., Kyoto Univ., No. 50 B, 2007

Evaluation of LNAPL Migration under Fluctuating Groundwater by Image Analysis

Giancarlo FLORES*, Takeshi KATSUMI* and Masashi KAMON*

*Graduate School of Global Environmental Studies, Kyoto University

Synopsis

This study assesses the suitability of an image analysis method as a tool to measure water and *light non-aqueous phase liquids* (LNAPLs) saturation distributions in whole domains, when evaluating the effects of groundwater fluctuations on LNAPL migration in the subsurface for fully saturated porous media. A logarithmic relation was found between average optical density (D_i) and saturation (S). The obtained correlation was used to analyze the behavior of a lowering groundwater table in a 3.5×3.5×50 cm one-dimensional column filled with Toyoura sand. Results showed that the image analysis method tested here provided with fairly good saturation distribution values for the whole system under dynamic conditions.

Keywords: LNAPL, image analysis, groundwater, contamination, column test

1. Introduction

Light non-aqueous phase liquids (LNAPLs), such as petroleum products, can pose significant contamination risks to the groundwater when released in the vadose zone. Efficient and cost-effective remediation of these releases should be guided by field data, which, in turn, should be interpreted by numerical models using the appropriate assumptions.

Modeling of multiphase flow requires that the constitutive relations between relative permeability (k), saturation (S) and pore pressure (p) of the fluids are known in order to solve the governing flow equations (Kechavarzi *et al.,* 2000). Of these three variables, saturation has proved to be the most elusive to deal with when working in dynamic environments, and modern non-intrusive non-destructive methods, such as gamma ray or conventional X-ray attenuation techniques, while expensive, do not allow the acquisition of dynamic fluid saturation distribution in entire domains at one time (Darnault *et al.,* 1998).

This study assesses the suitability of an image analysis method as a tool to measure water and light non-aqueous phase liquids (LNAPLs) saturation distributions in whole domains, when evaluating the effects of groundwater fluctuations on LNAPL migration in the subsurface for fully saturated porous media.

2. Image Analysis

The transmittance τ defines how much light is transmitted through a photographic negative and can be written as:

$$\tau = \frac{I_t}{I_o} \tag{1}$$

where I_t and I_o are the transmitted and incident luminous intensities, respectively.

The optical density D_t is related to the transmittance as:

$$D_t = -\log_{10}(\tau) \tag{2}$$

The average optical density D_i is defined for the

reflected light intensity as:

$$D_i = \frac{1}{N}\sum_{j=1}^{N} d_{ji} = \frac{1}{N}\sum_{j=1}^{N}\left(-\log_{10}\left(\frac{I_{ji}^{r}}{I_{ji}^{0}}\right)\right) \quad (3)$$

where N is the number of pixels contained in the area of interest and, for a given spectral band i, d_{ji} is the optical density of the individual pixels, I_{ji}^{r} is the intensity of the reflected light given by the individual pixel values, and I_{ji}^{0} is the intensity of the light that would be reflected by an ideal white surface (Kechavarzi *et al.,* 2000).

For this study, 50 different Toyoura sand samples were mixed with different amounts of blue-dyed water, and were immediately photographed with a consumer grade digital camera, Nikon D70s, using a 500 nm band-pass filter. A Kodak gray scale was located next to each sample to provide for a constant white reference, and a glass plate was placed over each sample. Great care was taken on including saturation values below 10% in order to account for the lower limits in drainage/imbibition processes. Final values ranged from 2% to 68%.

Pictures were analyzed with MATLAB R2006a, and the values for average optical density corresponding to each sample were calculated. Results are plotted in Fig. 1.

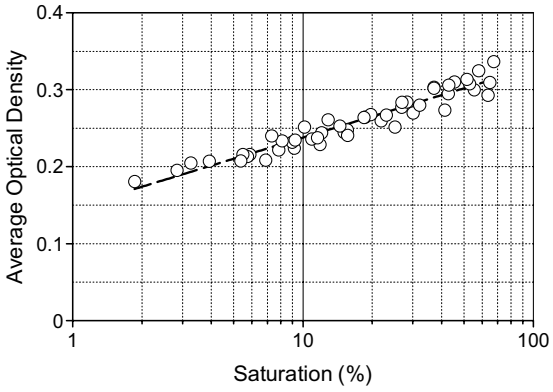

Fig. 1 Average optical density vs. saturation

A logarithmic relation was observed between average optical density and saturation:

$$\begin{cases} D_{500} = 0.0397 \ln S_w + 0.3293 \\ R^2 = 0.9233 \end{cases} \quad (4)$$

It was found (Fig. 2) that the effect of the blue dye (Brilliant Blue FCF, 1:10000) was an increase in the slope of the $D_i - S$ regression curve when plotted on a semi logarithmic chart, resulting in a more precise saturation estimation.

Pictures were taken to sixteen of samples with and without the top glass plate. It was found (Fig. 3) that the effect of the glass plate was a parallel displacement of the $D_i - S$ regression curve when plotted on the same semi-logarithmic chart.

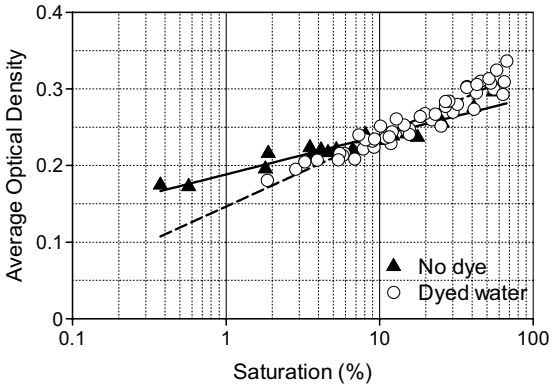

Fig. 2 Effect of blue dye on the slope of D_i-S curve

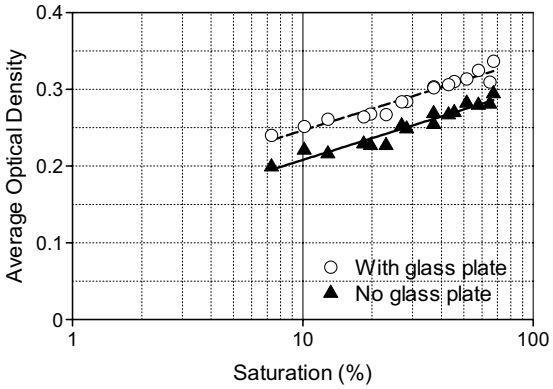

Fig. 3 Effect of the glass plate on the D_i-S curve

3. Air – Water Experiment

A 3.5×3.5×50 cm one-dimensional column with a transparent glass-wall (Fig. 4) was designed in order to study, with the help of the image analysis method tested previously, the behavior of a lowering groundwater table in a Toyoura sand column (Fig. 5).

The column was initially filled with fully saturated Toyoura sand. The water tank was quickly lowered 40 cm from its original position, to a height of 5 cm over the bottom of the column, and the water inside the column was let drain. The top of the column was let

open to avoid producing a vacuum effect. Digital pictures were taken following the frequency showed in Table 1. The camera was set to automatic mode. One 500 W floodlight was turned on 30 seconds before taking each picture, and was turned off right after it, to avoid changing the temperature of the column.

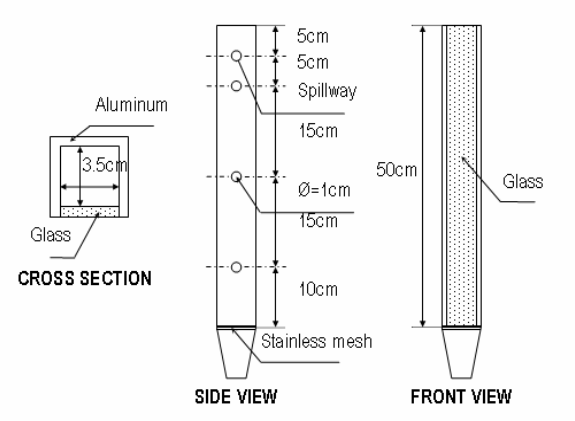

Fig. 4 Column design

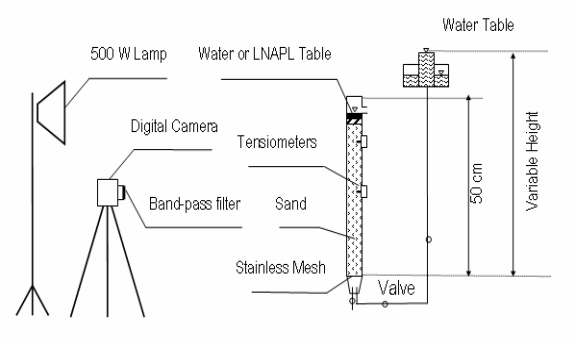

Fig. 5 Experimental system design

Table 1 Frequency for digital pictures

Hour	*Frequency*
0 to 0.5	1 min
0.5 to 2	5 min
2 to 4	10 min
4 to 6	30 min
6 to 12	1 hour
12 to 24	4 hours
24 to 32	8 hours

The values of average optical density for different heights were calculated. Results are plotted in Fig. 6.

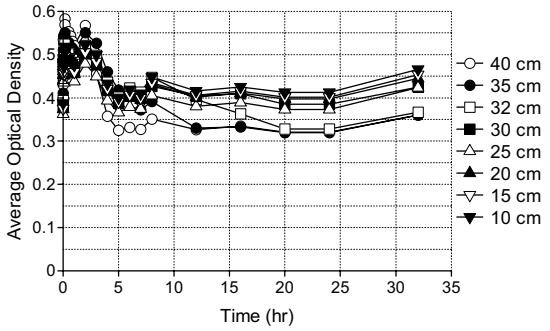

Fig. 6 Average optical density vs. time

To account for the effects of the variable external light during the experiment, which resulted in variable values of D_i for points that kept constant saturation values (e.g., h = 15 cm), the previous graphic was adjusted so that Di for h = 10 cm (the lower point analyzed, which was fully saturated during the whole experiment) was constant at all times (Fig. 7).

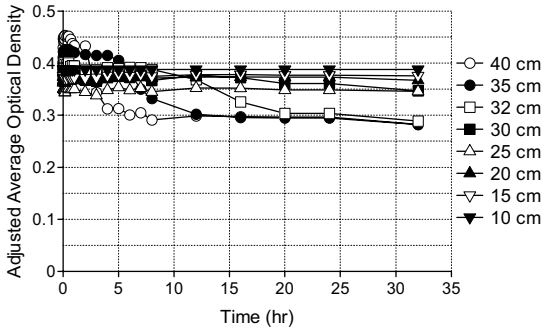

Fig. 7 Adjusted average optical density vs. time

To account for the effects of non-parallel light beams, which resulted in all points having different D_i values for t = 0 hr (even though the column was fully saturated at all heights), the differential in average optical densities (ΔD_i), referred to the picture taken at time t = 0 h, were calculated and plotted (Fig. 8).

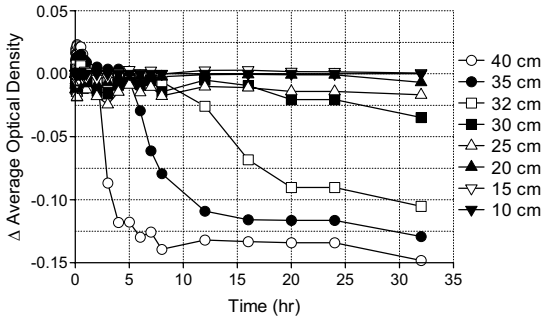

Fig. 8 Δ Average optical density vs. time

Using Equation (4) to calculate two different values of average optical density, subtracting one from the other, and operating, the following relation is obtained:

$$D_{500}^{1} - D_{500}^{0} = 0.0397 \ln\left(\frac{S_w^1}{S_w^0}\right) \quad (5)$$

Equation (5) is used to obtain saturation values (using $S_w^0 = 1$). The results are plotted in Fig. 9.

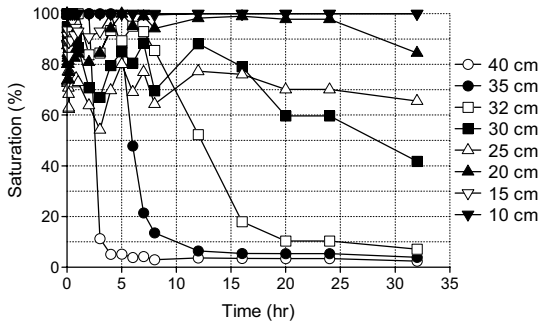

Fig. 9 Water saturation vs. time

The appearance of some inconsistencies during the analysis (e.g., higher saturation values on the top layers than on the bottom ones during the first hours) demonstrated that the method was highly sensitive to variations in lighting conditions. In order to minimize errors in next experiments, the following measures are suggested:

1. All external sources of light (doors and windows) should be sealed with opaque materials, and two floodlights instead of one should be used to minimize the effect of external light.
2. Camera should be set in manual mode so that aperture, shutter speed and white balance are kept constant during the whole experiment.
3. More than one gray scale should be located next to the column at different heights, to take into account the effect of non-parallel light beams.

4. LNAPL – Water Experiment

For this experiment, the column was filled again with fully saturated Toyoura sand. Two tensiometers, one hydrophilic and one hydrophobic, modified according to Kamon *et al.* (2003) and Kamon *et al.* (2007), were installed at mid-height to measure pore pressure. Preliminary experiments to obtain calibration curves were conducted prior to the column test, and they are shown in Fig. 10.

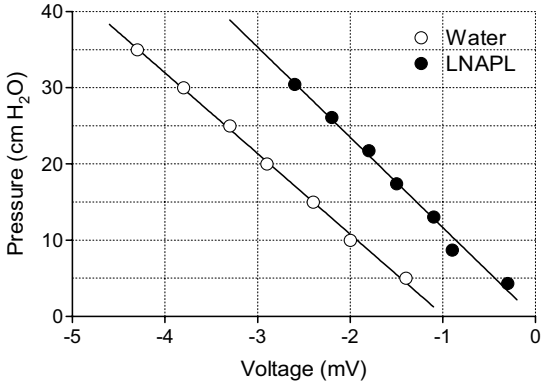

Fig. 10 Calibration curves of the tensiometers

The experiment was divided in two parts, drainage and imbibition, the first one from t = 0 hr to t = 72 hr, and the second one from t = 72 hr to t = 96 hr.

For the first part, the water tank was quickly lowered 40 cm from its original position to a height of 5 cm over the bottom of the column, and the water inside the column was let drain. LNAPL was infiltrated into the column from the top through the porous stone. Excess LNAPL drained through the spillway, which controlled the total height of the fluid table, assuring that the sand was kept fully saturated at all times. The top of the column was let open to avoid producing a vacuum effect. The drainage part of the experiment took 72 hours.

After the end of the drainage part, the water tank was quickly raised to a height of 74.3 cm over the bottom of the column and the water table inside the column moved up due to the upward water pressure. The LNAPL that infiltrated into the column during the drainage process was displaced by the water and flowed out of the column trough the top spillway. Water was infiltrated into the column from the bottom at the same rate as the LNAPL displacement, and the sand continued to be kept fully saturated at all times. The top of the column was let open to avoid producing overpressure. The imbibition part of the experiment took 24 hours.

During both parts, digital pictures were taken every 30 minutes. The camera was set to manual mode and all pictures were taken with the same aperture, shutter speed and white balance settings. Two 500 W floodlights were turned on 30 seconds before taking

each picture, and turned off 30 seconds after that, to avoid changing the temperature of the column.

The values of average optical density for several different heights were calculated. Results are plotted in Fig. 11. As in the first case, the curve was adjusted and allowed us to calculate the water saturation distribution over time. Since the column was fully saturated at all times, LNAPL saturation was calculated as the difference between 100% and water saturation (Fig. 12).

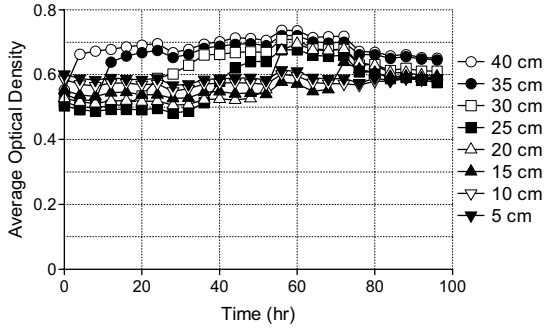

Fig. 11 Average optical density vs. time

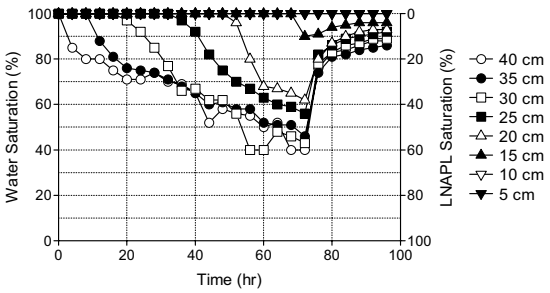

Fig. 12 Saturation vs. time

Fig. 12 depicts accurately the moments at which the LNAPL front crossed the analyzed points during the drainage process (i.e., the moments when water saturation drops from 100%). It can be noticed that the receding water front slowed over time, as can be seen by the increasingly larger periods of time that the LNAPL front needed to displace the water. This occurred due to the increase in pore pressure values (Fig. 13), which meant a decrease in the suction (negative pressure) of the receding water table.

The imbibition process seems to have two different slopes, a steep one the first 8 hours, and a moderate one the remaining 16 hours. It appears that this happens because at the beginning water can easily displace the pore entrapped LNAPL but, once LNAPL is reaching its residual saturation limit, water can not displace it as easily as before, and the process decelerates.

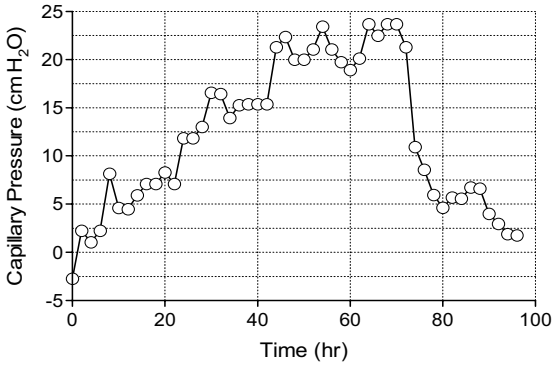

Fig. 13 Capillary pressure vs. time (h = 25 cm)

The overall results show that LNAPLs, despite being fluids with densities lower than water, might remain below the groundwater table, as residual LNAPL saturation, during imbibition processes.

Comparing capillary pressure vs. time (Fig. 13) as recorded by the tensiometers, and saturation vs. time (Fig. 12), it can be seen that water saturation and pore pressure have opposite behaviors: during the drainage process, while the water table fell and the water saturation of the sand decreased, the capillary pressure increased accordingly. Inversely, during the imbibition process, while the water table raised and the water saturation increased, the capillary pressure decreased. There is, in fact, a good correspondence among water saturation, capillary pressure and the water table displacement.

The water *S-p* relation is obtained by plotting together saturation and pore pressure values (Fig. 14). It can be seen that this relation follows different paths when in a drainage process or in an imbibition process, making it clear the hysteretic nature of the *S-p* relation.

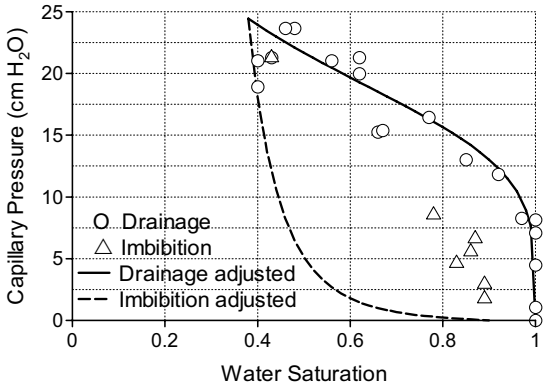

Fig. 14 *S-p* relation

The parameters of the fitting curve following the model developed by van Genuchten (1980) are reported in

Table 2, and the corresponding equations in Equation (6). They correspond nicely, for the drainage part (analysis not shown in this paper), to those reported by Li (2005) and Kamon *et al.* (2007) in a previous experiment.

$$\begin{cases} p_{drainage} = \dfrac{1.00}{0.05}\left(S^{-\frac{1}{1-1/4.50}} - 1 \right)^{\frac{1}{4.50}} \\ p_{imbibition} = \dfrac{0.89}{5.00}\left(S^{-\frac{1}{1-1/1.18}} - 1 \right)^{\frac{1}{1.18}} \end{cases} \quad (6)$$

Table 2 Fitted parameters of the *S*-*p* VG model

	α	n	S_{wi}	S_{wr}
Drainage	0.05	4.50	1.00	0.17
Imbibition	5.00	1.18	0.89	0.17

From the saturation vs. time data (Fig. 12), the total amount of infiltrated LNAPL at t = 72 h was calculated as 149.74 ml (analysis not shown in this paper). The real amount of infiltrated LNAPL, as registered during the experiment, was 138.01 cm^3. This means that the volumetric error, as calculated by this method, was less than 10%.

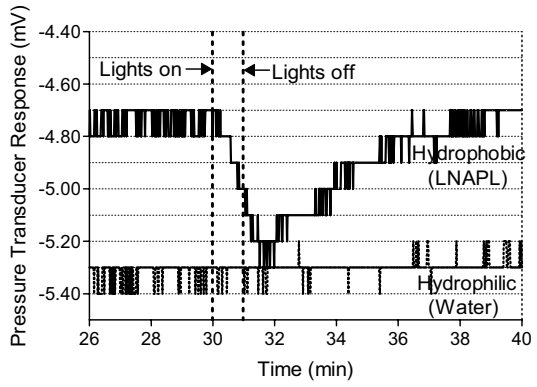

Fig. 15 Tensiometers response to 500 W lamps

During the study it was found that the hydrophobic tensiometers were affected by the external light. As can be seen in Fig. 15, the voltage reported by the hydrophobic tensiometer (LNAPL) dropped right after the lamps were turned on (in this case, at t = 30 min), kept dropping for 30 seconds after the lights were turned off (t = 31 min), and then slowly recovered for 7 – 8 minutes. The voltage reported by the hydrophilic tensiometer (Water) showed no change.

It appears that the small amount of LNAPL that was introduced in the shaft as part of our process to transform a hydrophilic tensiometer into a hydrophobic one (Kamon *et al.,* 2003; Li 2005; Kamon *et al.,* 2007) has a large coefficient of thermal expansion. This would have caused the LNAPL to expand after heated by the light beams, increasing the pressure in the shaft which was interpreted by the tensiometer as an increase in external pressure. According to Fig. 10, increases in pressure are reported by the tensiometer as displacements in voltage values to the negative side, which is what can be seen in Fig. 15.

It is recommended for future experiments that require these modified tensiometers, to protect them from external light sources to avoid incorrect pressure measurement.

5. Conclusions

This study analyzed the suitability of an image analysis method to assess water and LNAPL saturation values in porous media under fluctuating groundwater conditions, as a tool to be used for environmental geotechnical studies on the mechanisms of LNAPL migration in subsurface.

A logarithmic relation was found between average optical density and saturation for different soil samples, when including in the analysis saturation values as low as 2%. This equation allowed us to calculate water saturation distribution over time in a porous medium one-dimensional column, in two different two-phase experiments (air-water and LNAPL-water) which, in turn, permitted us to study the fate of a LNAPL as contaminant, when faced to a fluctuating groundwater table.

The study confirmed the expected behavior that LNAPLs in occasions remain below the groundwater table, as residual LNAPL saturation, during imbibition processes.

The results obtained by the image analysis method reviewed here demonstrated that this technique, while relative inexpensive, provides with fairly good information about the water saturation distribution over time in an entire column domain, for air-water and LNAPL-water two-phase systems.

References

Darnault, C.J.G., Throop, J.A., DiCarlo, D.A., Rimmer, A., Steenhuis, T.S. and Parlange, J.Y. (1998): Visualization by Light Transmission of Oil and Water Contents in Transient Two-Phase Flow Fields, Journal of Contaminant Hydrology, 31, 337-348.

Kamon, M., Endo, K. and Katsumi, T. (2003): Measuring the k-S-p Relations on DNAPLs Migration, Engineering Geology, 70, 351-363.

Kamon, M., Li, Y., Endo, K., Inui, T. and Katsumi, T. (2007): Experimental Study on the Measurement of S-p Relations of LNAPL in a Porous Medium, Soils and Foundations, 47 (1), 33-45.

Kechavarzi, C., Soga, K. and Wiart, P. (2000): Multispectral Image Analysis Method to Determine Dynamic Fluid Saturation Distribution in Two-Dimensional Three-Fluid Phase Flow Laboratory Experiments, Journal of Contaminant Hydrology, 46, 256-293.

Li, Y. (2005): Mechanism of LNAPL Migration in Conjunction with Groundwater Fluctuation, Doctoral Thesis, Kyoto University, Kyoto, Japan.

Van Genuchten, M.T. (1980): A Closed-Form Equation for Predicting the Hydraulic Conductivity of Unsaturated Soils, Soils Science Society of America Journal, 44 (5), 892-898.

画像解析手法を用いた地下水位変動条件下におけるLNAPL挙動の評価

Giancarlo FLORES*・勝見　武**・嘉門雅史**

*京都大学大学院地球環境学舎
**京都大学大学院地球環境学堂

要　旨

本論文は，水とLNAPL（light non-aqueous phase liquids）の飽和度分布を測定するための画像解析法の適用性を検討したものであり，地下水位が変動する条件下でのLNAPLの移動特性の解明を目指している。まず，平均光密度と飽和度の間の対数相関関係を明らかにした。次に，この関係を使って3.5×3.5×50 cmの豊浦砂一次元カラムで地下水位が変動する条件での実験を行った。実験を行った結果，本研究で用いた画像解析の手法を用いることにより，動的条件下における土中の飽和度を測定できることが明らかとなった。

キーワード: LNAPL，画像解析，地下水，汚染，カラム試験